Review Article ISSN 2771-666X

Journal of Advanced Materials Science and Engineering

Density Functional Theory Study of Lithium Polysulfide Conversion in Co4N Doped Lithium Sulfur Battery System

Shiming Li[1] and Daoling Peng[2]*

[1]*School of Chemistry, South China Normal University, Guangzhou 510006, China.*

[2]*Key Laboratory of Theoretical Chemistry of Environment, Ministry of Education, School of Environment, South China Normal University, Guangzhou 510006, China.*

***Correspondence:**
Daoling Peng, Key Laboratory of Theoretical Chemistry of Environment, Ministry of Education, School of Environment, South China Normal University, Guangzhou 510006, China.

Received: 01 Feb 2024; **Accepted:** 12 Mar 2024; **Published:** 18 Mar 2024

Citation: Shiming Li, Peng D. Density Functional Theory Study of Lithium Polysulfide Conversion in Co4N Doped Lithium Sulfur Battery System. J Adv Mater Sci Eng. 2024; 4(1): 1-6.

ABSTRACT

Lithium-sulfur (Li-S) batteries are widely considered to be one of the most promising next-generation energy-storage systems due to its high theoretical energy density. But there are still some problems, including of the shuttling of lithium polysulfides (LiPSs; Li_2S_n, n=2, 4, 6 or 8) and sluggish decomposition of solid Li_2S, seriously hinder its practical application. Since Co_4N has showed its capability to alleviate shuttle effect and accelerate electrode reactions kinetics on S cathode, which can effectively improve Li-S batteries performance. We theoretically investigated the adsorption properties and conversion mechanisms of the LiPSs species on the $Co_4N(111)$ surface by the first-principle density functional theory (DFT) calculations. Both the electronic structures of LiPSs and the chemical and physical properties of Co_4N were studied. The free energy pathway of Li_2S decomposition on the considered surface was modeled by a suggested stepwise cathodic delithium reaction mechanism. A series of transition state structures were obtained and low barrier energies were found, indicating that Co_4N could be a good candidate for the research of lithium-sulfur batteries.

Introduction

To meet the growing demand for increased driving range in electric vehicles, more and more attention has been focused on lithium-sulfur (Li-S) batteries, whose theoretical energy density (2600 $Wh \cdot kg^{-1}$) [1] is much higher than traditional lithium ion batteries (about 400 $Wh \cdot kg^{-1}$) [2]. However, there still exist some obstacles in its commercial application: the shuttle effect caused by lithium polysulfides (LiPSs), the large decomposition energy of Li_2S, the poor cycle life arising from the insulating property of S and Li_2S, low utilization of cathodic active components, passivation of the lithium electrode [3,4], poor rate capability [5] and severe volume change during cycling [6]. In order to tackle the aforementioned concerns, a series of carbon-based materials and metal-based materials use sulfur as host material to confine LiPSs by physical or chemical interaction. Carbon-based materials include porous carbon [7-9], hollow carbon [10-12], wood-derived carbon [13], carbon nanofiber and carbon nanotube [14]. Metal-based materials are MXene [5] and transition metal oxides/nitrides/sulfides [15-19]. It was also useful to place separators that can adsorb LiPSs between the electrodes, such as Co_4N-Celgard separator [20], LiPS/N-CDs clotting layer [6] and p-Fe_3O_4-NSs-based separator [21]. In addition to experimental tests, theoretical first-principle density functional theory (DFT) calculations were also carried out to gain an in-depth understanding for the adsorption process of LiPSs, Li_2S decomposition and Li diffusion on different substrates. Calculations show that 1.21 eV is the barrier energy for $Li_2S \rightarrow LiS + S$ on Co-N_4 (a single Co atom bonded to four pyridinic N) [22], 0.32 eV is the activation barrier energy for $Li_2S_4 \rightarrow Li_2S + S_3$ on 1T-MoS2-1S [23], 1.19 eV is the barrier energy for Li_2S decomposition on V_2NS_2 [24] and Fe/N doped carbon has 0.035 eV as the barrier energy for Li ion diffusion due to the pyridinic nitrogen [25]. Among these materials, Co_4N exhibited its capability to alleviate LiPSs shuttling and accelerate the conversion of multiple redox during cycling. However, the conversion mechanism with Li_2S as the initial reactant on the surface of Co_4N has not been reported. Thus, we theoretically investigated the adsorption process, reaction mechanism of the conversion of

multiple sulfur species, Li_2S decomposition, S atom diffusion on the surface of Co_4N by first-principle DFT calculations.

Results and Discussions

Adsorption

Since the DFT calculations are very time consuming, a relative lower cost DFT tight-binding (DFTB) method was employed for pre-DFT calculations. This reduce the number of iterative steps in the subsequent DFT calculations. DFTB+ program was used for rough geometry optimization with convergence criterion of 1×10^{-8} eV for energy [26]. First-principle DFT calculations were carried out by the Vienna ab initio simulation package (VASP) [27,28]. The projector augmented wave potentials (PAW) [29] and the generalized gradient approximation (GGA) with Perdew–Burke–Ernzerhof functional (PBE) [30] were employed in DFT calculations. After the convergence test of energy cutoff parameters, the plane wave basis set with cutoff energy of 600 eV was used. The convergence criterion of 1×10^{-8} eV and 2×10^{-2} eV/Å for energy and force were used during geometric optimizations. A vacuum space of 12 Å was constructed in the slab model of $Co_4N(111)$ surface to avoid the interactions between periodic images. The Brillouin zones were sampled with 2 × 2 × 1 Gamma–center meshes.

The adsorption substrate was constructed by a four layers model. As illustrated in Figure 1a, the Co and N atom layers were placed in a sequence of Co-N-Co-N. The Co is placed in the outmost layer since the interaction with sulfur atom is stronger than the nitrogen atom. The adsorbates (sulfur, lithium sulfide and LiPSs) and their adsorption configurations on $Co_4N(111)$ surface were showed in Figure 1b and 1c, respectively. Some of the initial structures were taken from the work by Wang [5], the others (Li_2S_6 and Li_2S_8) were gained by the global searching results using ABCluster [31]. All geometry structures were optimized by DFT calculations and no imaginary vibration frequencies were found, indicating all molecules are in stable conformations.

The anchoring effect for above adsorbates of $Co_4N(111)$ surface was evaluated by calculating the adsorption energies (E_{ad}) according to the following equation,

$$E_{ad} = E_{adsorbate} + E_{Co4N(111)} - E_{*adsorbate} \quad (1)$$

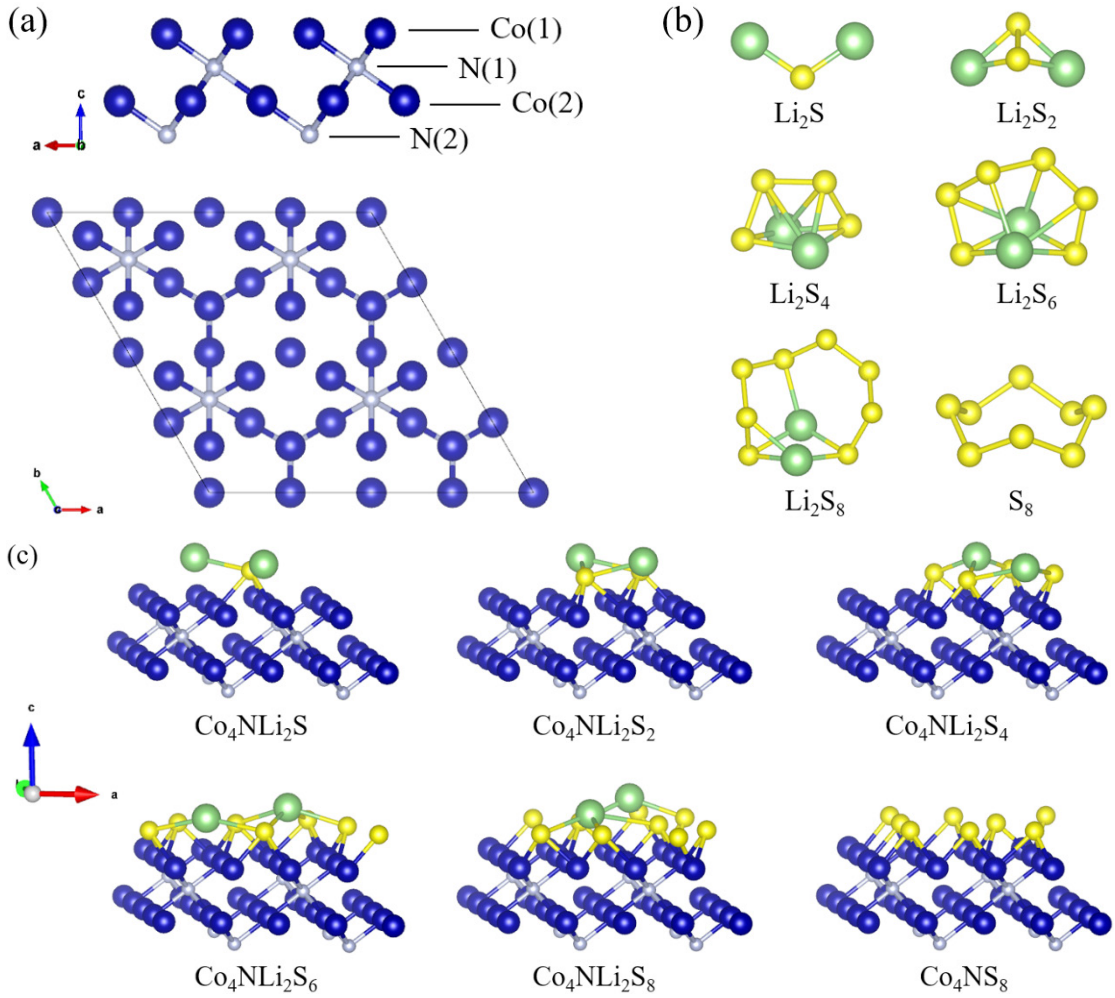

Figure 1: (a) Side and top view of $Co_4N(111)$ surface; (b) Diagrams of Li_2S, Li_2Sn and S_8 structures; (c) Adsorption configurations of Li_2S, Li_2Sn and S_8 on $Co_4N(111)$ surface.

where $E_{Co4N(111)}$ and $E_{*adsorbate}$ are the total electronic energies of $Co_4N(111)$ without/with above adsorbates, respectively. $E_{adsorbate}$ is the total electronic energy of each adsorbate itself.

Our calculated results showed that $Co_4N(111)$ surface had considerable affinity for all of these lithium sulfur species with adsorption energies ranging from 5.344 eV to 20.144 eV during the whole delithiation process (Figure 2a), indicating that Co_4N can not only effectively suppress the dissolution and shuttling process of LiPSs but also accelerate the Li_2S multiple delithiation process. Anyway, due to the strong adsorption strength, most of the S-S bond in adsorbates were broken and then S atoms dispersed to the surface of $Co_4N(111)$, while the Li atoms are still bonded with S atoms.

The calculated total density of states (DOS) show that Co_4N still retain metallic conductivity after adsorption (Figure 2b), which can improve the low utilization of cathodic active components. The calculated charge density difference showed that electron-rich regions (yellow) generally appear between S and Co after adsorption, indicating the formation of new polar S-Co bonds (Figure 2c). This also revealed that the adsorption energies after delithiation were increased except for S_8 and the high adsorptive strength of Co_4N can be attributed to the chemical interaction with adsorbates. Meanwhile, Li-S bonds in adsorbates were weaken in the electron-deficient regions (blue) which appeared between Li and S. It might be beneficial to the departure of Li.

Reaction Path

In order to find the minimum energy path of the conversion of multiple delithiation on the surface of $Co_4N(111)$, the climbing-image nudged elastic band (CI-NEB) method [32] was employed with an IDPP path as the initial path [33]. VASPKIT 1.3.5 [34] software was used to calculate Gibbs free energy correction for the molecules adsorbed on the substrate.

For Gibbs free energy calculations, we made use of the following reaction sequence to illustrate the delithiation process: $Li_2S \rightarrow Li_2S_2 \rightarrow Li_2S_4 \rightarrow Li_2S_6 \rightarrow Li_2S_8 \rightarrow S_8$. The specific calculations of barrier energies with four sub-steps were expressed as follows:

$$G_{*Li_2S_2}{}^{\ddagger} - G_{*Li_2} - 2G_{*S} \quad (2)$$

$$G_{*Li_2S_4}{}^{\ddagger} - G_{*Li_2S_2} - 2G^*_S \quad (3)$$

$$G_{*Li_2S_6}{}^{\ddagger} - G_{*Li_2S_4} - 2G_{*S} \quad (4)$$

$$G_{*Li_2S_8}{}^{\ddagger} - G_{*Li_2S_6} - 2G_{*S} \quad (5)$$

where $G_{*adsorbate}{}^{\ddagger}$ and $G_{*adsorbate}$ were the Gibbs free energies of the transition state and ground state of $Co_4N(111)$ together with adsorbates, respectively. G_{*S} (-6.887 eV) was the average Gibbs free energy of single S atom adsorbed on the same substrate in three configurations as illustrated in Figure 3a.

As illustrated in Figure 3b, the delithiation step of transforming

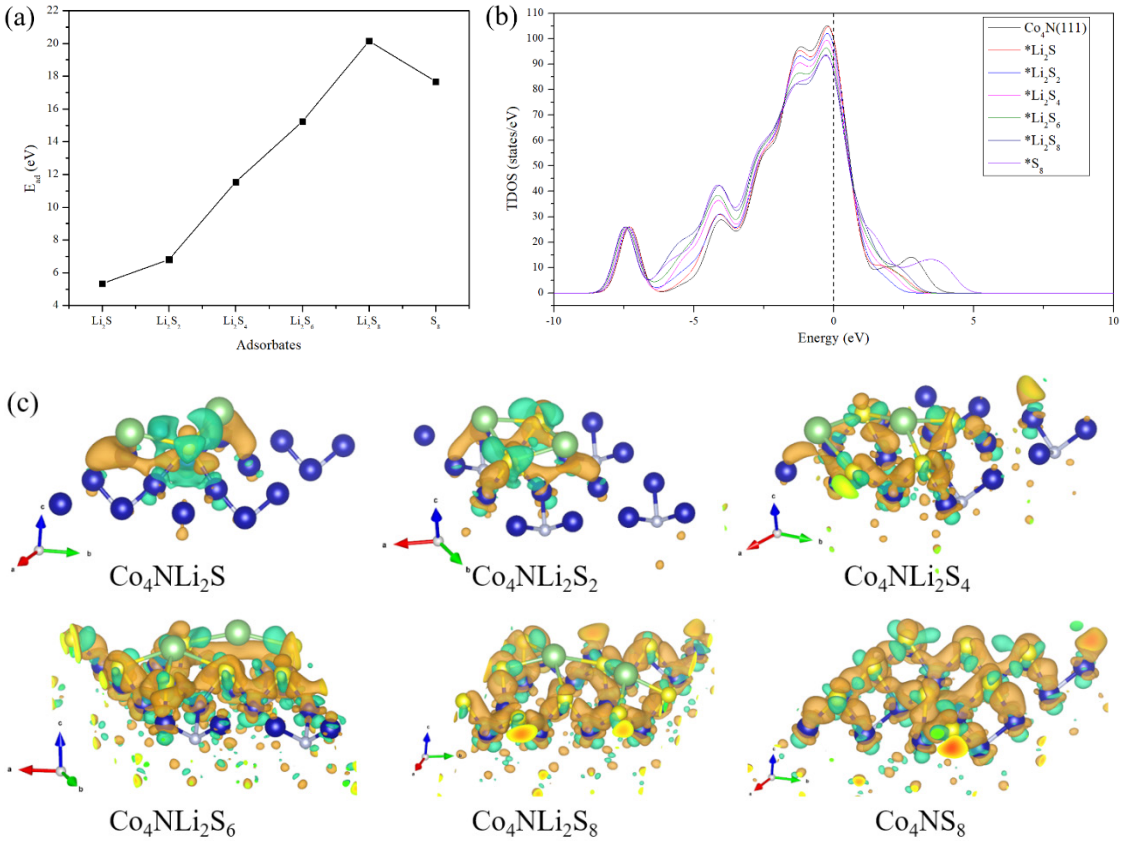

Figure 2: (a) Adsorption energies of Li_2S, Li_2Sn and S_8 on $Co_4N(111)$; (b) Total density of states before and after adsorptions; (c) Charge density difference of Li_2S, Li_2Sn and S_8 on $Co_4N(111)$.

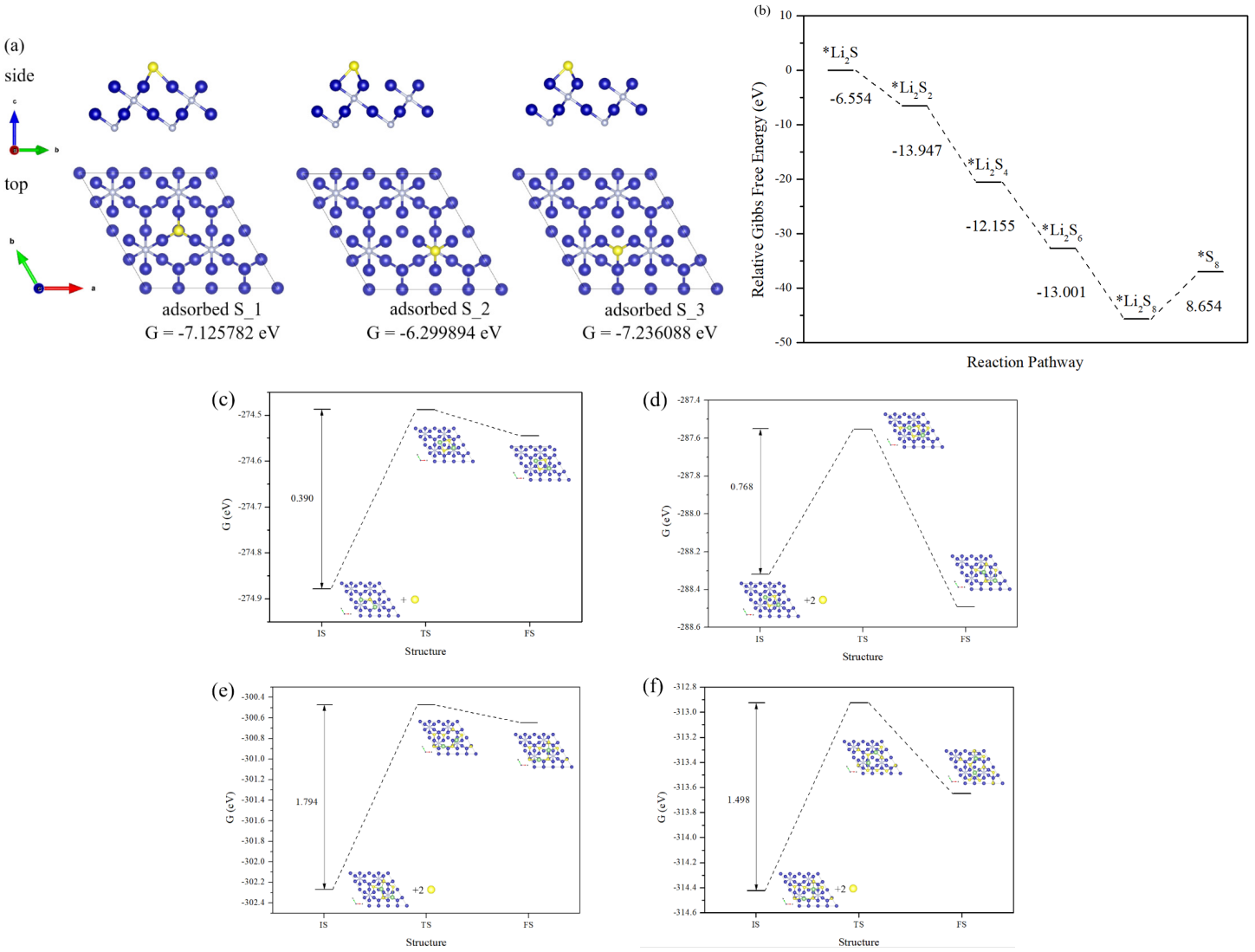

Figure 3: (a) Side and top views of three adsorption configurations of single S atom and it's Gibbs free energies; (b) The energy profiles for the delithiation of Li_2S and LiPSs on $Co_4N(111)$; (c)~(f) The energy profiles of $Li_2S \rightarrow Li_2S_2$, $Li_2S_2 \rightarrow Li_2S_4$, $Li_2S_4 \rightarrow Li_2S_6$ and $Li_2S_6 \rightarrow Li_2S_8$, respectively.

Li_2S to Li_2S_8 is a spontaneous exothermic reaction on the substrate, whereas the step of transforming Li_2S_8 to S_8 is endothermic. From Li_2S to Li_2S_8, all free energy changes of adjacent species are negative. The smallest free energy change occurs in the $Li_2S \rightarrow Li_2S_2$ step with a value of -6.554eV, and the largest free energy change happens in the $Li_2S_2 \rightarrow Li_2S_4$ step with a value of -13.497 eV. However, free energy change becomes positive in the final $Li_2S_8 \rightarrow S_8$ step.

Since the thermodynamic results do not reflect the degree of difficulties of each reaction steps, we calculated the kinetic data by the help of transition state theory. As shown in Figure 3c-3f, four transition states were obtained by using the CI-NEB method, and the free energy differences between transition states (TS) and initial states (IS) are evaluated as activation free energy barriers. The final state (FS) is the initial state of the subsequent step. The lowest free energy barrier was found in the $Li_2S \rightarrow Li_2S_2$ step with a value of 0.390 eV. The rate-limiting step has the largest free energy barrier which take place in the $Li_2S_4 \rightarrow Li_2S_6$ step exhibited an energy barrier of 1.794 eV, since this step require the breaking of Li-S bond. The other steps exhibited relatively small barrier energies in a range of 0.390 eV to 1.498 eV. S diffusion and Li_2S decomposition on the same surface which may infect the reaction kinetics were also taken into considered.

As shown in Figure 4a, the decomposition barrier of Li_2S adsorbed on $Co_4N(111)$ was decreased from 3.390 eV to 0.226 eV, which was also small compared to other substrates such as Co_{13} [22] cluster and Co-N co-doped carbons [35]. The small barrier energy of Li_2S decomposition reflects that the moving of Li atom on the substrate would not be difficult. For S atom diffusion on the same substrate, the energy barrier is 0.293 eV as can be seen in Figure 4b. It was small enough compared to the barrier energy of sulfur species conversion, indicating that it would not be the obstacle of Li_2S delithiation. The detailed diffusion pathway of the S atom was demonstrated in Figure 4c. The initial state of S atom was place in the top position of nitrogen atom, and the final state was moved to the hole with Co surrounding. The diffusion path is obviously

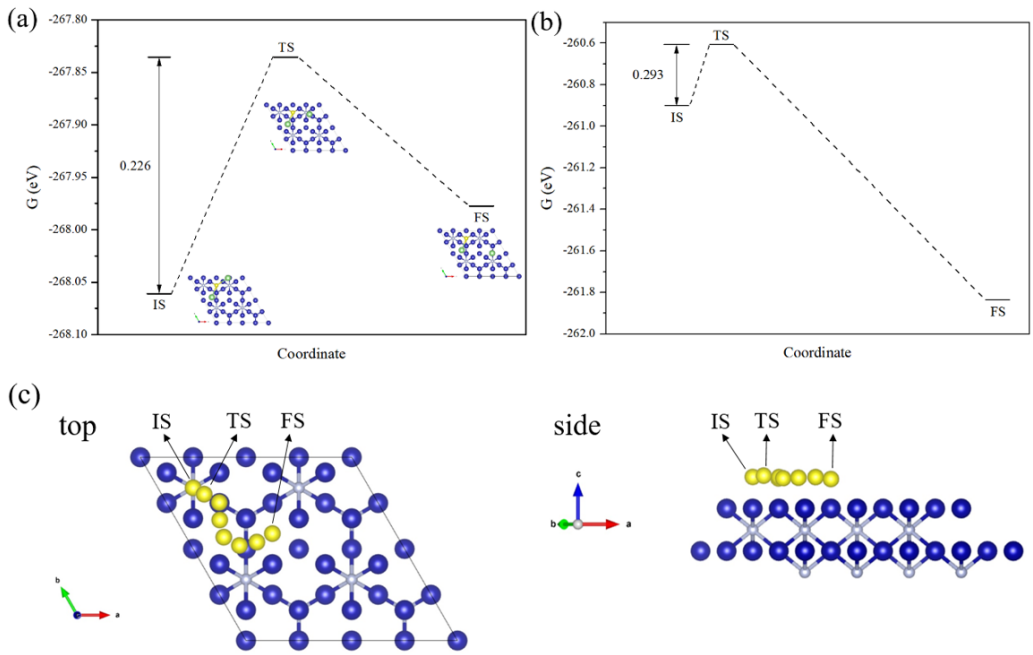

Figure 4: The energy profiles of (a) the decomposition of Li_2S and (b) S diffusion on $Co_4N(111)$; (c) side and top views of S diffusion on $Co_4N(111)$.

not straight line, since the top position of the Co atom has high potential energy to avoid the confliction of Co and S atom. The transition state is closer to the initial state since the final state has large energy difference while initial state has small energy difference.

Conclusions

We theoretically investigated the adsorption and conversion mechanisms of the lithium-sulfur species on the surface of $Co_4N(111)$ by the first-principle density functional theory (DFT) calculations. The chemical affinity for LiPSs and electro-catalytic ability of Co_4N were proved by the calculated large adsorption energy ranging from 5.344 eV to 20.144 eV and the extremely decreased barrier energy of Li_2S decomposition process. In addition, we also studied the free energy pathway of stepwise cathodic delithium reactions and S atom diffusion on the considered surface. A series of transition state structures and barrier energies in the range of 0.293 eV to1.794 eV were obtained.

In summary, Co_4N can accelerate the delithiation reaction after adsorbing sulfur species. Notably, the rate-determining step of Li_2S stepwise delithiation is the $Li_2S_4 \rightarrow Li_2S_6$ step which has the barrier energy of 1.794 eV due to the breaking of Li-S bond.

Acknowledgement

The authors would like to thank the National Key Research and Development Program of China (2017YFB0203403) for financial support.

References

1. Mikhaylik YV, Akridge JR. Polysulfide Shuttle Study in the Li/S Battery System. J Electrochem Soc. 2004; 151: A1969-A1976.
2. Janek J, Zeier WG. A Solid Future for Battery Development. Nat Energy. 2016; 1: 16141.
3. Wei Z, Ren Y, Sokolowski J, et al. Mechanistic understanding of the role separators playing in advanced lithium-sulfur batteries. Infomat. 2020; 2: 483-508.
4. Manthiram A, Fu Y, Chung SH, et al. Rechargeable Lithium–Sulfur Batteries. Chem Rev. 2014; 114: 11751-11787.
5. Wang D, Li F, Lian R, et al. A General Atomic Surface Modification Strategy for Improving Anchoring and Electrocatalysis Behavior of Ti3C2T2 MXene in Lithium–Sulfur Batteries. ACS Nano. 2019; 13: 11078-11086.
6. Fu Y, Wu Z, Yuan Y, et al. Switchable Encapsulation of Polysulfides in the Transition between Sulfur and Lithium Sulfide. Nat Commun. 2020; 11: 845.
7. Schuster J, He G, Mandlmeier B, et al. Spherical Ordered Mesoporous Carbon Nanoparticles with High Porosity for Lithium-Sulfur Batteries. Angew Chem Int Ed Engl. 2012; 51: 3591-3595.
8. Yoshida L, Hakari T, Matsui Y, et al. Polyglycerol-functionalized microporous carbon/sulfur cathode for Li-S battery. Electrochimica Acta. 2022; 429: 141000.
9. Rayappan PR, Babu MP, Murugan R, et al. Confined sulfur electrode to achieve quasi-solid state sulfur conversion reaction in Li-S battery. J Energy Storage. 2023; 67: 107601.
10. Sun Z, Vijay S, Heenen HH, et al. Catalytic Polysulfide Conversion and Physiochemical Confinement for Lithium–Sulfur Batteries. Adv Energy Mater. 2020; 10: 1904010.
11. Su L, Zhang J, Chen Y, et al. Cobalt-embedded hierarchically-porous hollow carbon microspheres as multifunctional confined reactors for high-loading Li-S batteries. Nano Energy. 2021; 85: 105981.

12. He J, Jiao L, Cheng X, et al. Structural Regulation of Metal Organic Framework-derived Hollow Carbon Nanocages and Their Lithium-Sulfur Battery Performance. Acta Chimica Sinica. 2022; 80: 896-902.
13. Zhang W, Xu B, Zhang L, et al. Co4N-Decorated 3D Wood-Derived Carbon Host Enables Enhanced Cathodic Electrocatalysis and Homogeneous Lithium Deposition for Lithium–Sulfur Full Cells. Small. 2022; 18: 2105664.
14. Dai X, Lv G, Wu Z, et al. Flexible Hierarchical Co-Doped NiS2@CNF-CNT Electron Deficient Interlayer with Grass-Roots Structure for Li-S Batteries. Adv Energy Mater. 2023; 13: 2300452.
15. Wang X, Li G, Li J, et al. Structural and chemical synergistic encapsulation of polysulfides enables ultralong-life lithium–sulfur batteries. Energy Environ Sci. 2016; 9: 2533-2538.
16. Hai B, Ma L, Yan H, et al. In-Situ Synthesis of Sulfur-TiO2 Hollow Shell Materials for High-Performance Lithium-Sulfur Batteries. IOP Conf Ser.-Earth Environ Sci. 2017; 64: 012096.
17. Mosavati N, Salley SO, Ng KYS. Characterization and electrochemical activities of nanostructured transition metal nitrides as cathode materials for lithium sulfur batteries. J Power Sources. 2017; 340: 210-216.
18. Deng D, Xue F, Jia Y, et al. Co4N Nanosheet Assembled Mesoporous Sphere as a Matrix for Ultrahigh Sulfur Content Lithium–Sulfur Batteries. ACS Nano. 2017; 11: 6031-6039.
19. Zhao S, Kang D. The electrochemical performance investigation of cobaltous sulfides as host materials in advanced energy storage system. Ionics. 2021; 27: 3035-3039.
20. Pu J, Wu J, Tan Y, et al. Cobalt Nitride Nanocrystals Coated Separator as Multifunctional Interlayer for Improving Polysulfides Regulation. J of Alloys and Compounds. 2022; 920: 165964.
21. Zhang X, Yuan W, Huang H, et al. Rational design and low-cost fabrication of multifunctional separators enabling high sulfur utilization in long-life lithium-sulfur batteries. Int J Extrem Manuf. 2023; 5: 015501.
22. Zhou X, Meng R, Zhong N, et al. Size-Dependent Cobalt Catalyst for Lithium Sulfur Batteries: From Single Atoms to Nanoclusters and Nanoparticles. Small Methods. 2021; 5: 2100571.
23. Hojaji E, Andritsos EI, Li Z, et al. DFT Simulation-Based Design of 1T-MoS2 Cathode Hosts for Li-S Batteries and Experimental Evaluation. Int J Mol Sci. 2022; 23: 15608.
24. Fan K, Ying Y, Luo X, et al. Nitride MXenes as sulfur hosts for thermodynamic and kinetic suppression of polysulfide shuttling: a computational study. J Mater Chem A. 2021; 9: 25391-25398.
25. Huang X, Ren Y, Long J, et al. Promoted redox chemistry of high sulfur content cathode via endowing fast Li-ion diffusion. Ionics. 2022; 28: 1473-1481.
26. Hourahine B, Aradi B, Blum V, et al. DFTB+, a software package for efficient approximate density functional theory based atomistic simulations. J Chem Phys. 2020; 152: 124101.
27. Kresse G, Hafner J. Ab initio molecular dynamics for open-shell transition metals. Phys Rev B Condens Matter. 1993; 48: 13115-13118.
28. Kresse G, Furthmuller J. Efficient iterative schemes for ab initio total-energy calculations using a plane-wave basis set. Phys Rev B Condens Matter. 1996; 54: 11169-11186.
29. Blochl PE. Projector augmented-wave method. Phys Rev B. 1994; 50: 17953-17979.
30. Perdew JP, Burke K, Ernzerhof M. Generalized Gradient Approximation Made Simple. Phys Rev Lett. 1996; 77: 3865-3868.
31. Zhang J, Dolg M. ABCluster: The artificial bee colony algorithm for cluster global optimization. Phys Chem Chem Phys. 2015; 17: 24173-24181.
32. Henkelman G, Uberuaga BP, Jonsson H. A climbing image nudged elastic band method for finding saddle points and minimum energy paths. J Chem Phys. 2000; 113: 9901-9904.
33. Smidstrup S, Pedersen A, Stokbro K, et al. Improved initial guess for minimum energy path calculations. J Chem Phys. 2014; 140: 214106.
34. WangV, Xu N, Liu JC, et al. VASPKIT: A user-friendly interface facilitating high-throughput computing and analysis using VASP code. Comput Phys Commun. 2021; 267: 108033.
35. Ye H, Sun J, Zhang S, et al. Stepwise Electrocatalysis as a Strategy against Polysulfide Shuttling in Li–S Batteries. ACS Nano. 2019; 13: 14208-14216.